ID 1099

AXIAL ENERGY ABSORPTION OF SANDWICHED COMPOSITE TUBES

Qiang Yuan, Lin Ye and Yiu-Wing Mai

Centre of Advanced Materials Technology, School of Aerospace, Mechanical and Mechatronic Engineering, The University of Sydney, NSW 2006, Australia

SUMMARY: Sandwiched tubes were made with shell from pultruded tubes and polyurethane foam as a core. Both sandwiched and pultruded tubes were machined into the bevel or tulip shape and crushed in the axial direction. The crushing processes of the sandwiched tubes were more stable than the pultruded tubes. Specific energy absorption of the sandwiched tube is higher than the pultruded tubes with the machines bevels. Different machined shapes of sandwiched tubes have less effect on the specific energy absorption. Rigid foam restricted the bending deformation of the shell layer and led to more fracturing of the shell tubes. If the foam layer was too thick, large delamination was found between the foam and the shell.

KEYWORDS: Sandwiched Tube, Pultruded Tube, Crush, Energy Absorption

INTRODUCTION

Fibre reinforced composite materials are applied more and more extensively in the automobile and helicopter structures, due to their high strength and low density. One of the most important requirements for such applications is their energy absorbing capability in a controlled manner under crushing conditions [1-2].

To increase the specific energy absorbing ability many studies have been done using different fibre configurations and matrix systems [3-13]. On the other hand, the geometry shape of structure also plays an important role. Different triggered pultruded tubes have been investigated [14-16]. The tulip triggered tube showed higher specific energy absorption capability than the bevel triggered tube.

Pultrusion is a continuous processing method suitable to manufacture a large product amounts. Crushing behaviour of these pultruded glass fibre reinforced polyester and poly-vinyl-ester tubes have been studied at a high strain rate [17]. The specific energy absorption at the 12m/s was 20% more than in the quasi-static test. Czaplicki et. al. studied crushing behaviour of the E-glass fibre/polyester pultruded tubes in the non-axial loading configuration [18]. The maximum crush load decreased with the angle of inclination, and the energy absorption in the non-axial loading was less than in the axial loading, since the fibre orientation was not alone the crush load direction [19].

For a tube with large diameter and thin wall thickness, the crush processing is usually unstable and easily results in buckling failure, which reduces energy absorption ability. To increase the stability of the crush and the energy absorption capability, Gupta et. al. used a soft foam to fill in the composite tube [19]. The compression strength and crush stability were increased for the filled tube. Wei [20-21] designed a sandwiched tube which consisted of the two concentric steel tubes with polymer foam between the two tubes. The crush behaviour of this sandwiched tube appeared to have higher energy absorption and less buckling failure.

This work focused on the crush properties of the polymer sandwiched tubes, which consisted of two pultruded tubes as shells and polyurethane foam as a core. Different geometric dimensions and triggered shapes were studied. The specific energy absorption ability and failure modes were evaluated.

EXPERIMENTAL

Materials

The pultruded tubes consisted of a glass fibre reinforced polyester with a glass fibre content of 55 wt%, supplied by Pacific Composite Pty, Ltd. Australia. In the surface layer of tube, the fibre configuration is a continuous glass strand mat, while in the middle the orientation of the fibre is unidirectional. The outside square length of the tubes was 51 mm (T1), 38 mm (T2) and 25 mm (T3), respectively, and all tubes have the same wall thickness (3.2 mm).

Three types of the sandwiched tubes, (named as ST1, ST2, ST3), were made from the pultruded tubes T1-T2, T1-T3, and T2-T3 as shell layers and polyurethane foam as a core. To make the sandwiched tube two pultruded tubes were fixed alone the axial symmetry with screws, and one end of the tubes was sealed with an adhesive film. A mixture of polymeric isocyanates (Suprasec 2085, ICI) and polyether polyols (Daltolac SF7, ICI), with a weight ration of 87:100, was poured between two tubes until one third of the capacity. The other end of the tubes was sealed, and the tube assembly was laid horizontally. After 30 minutes, the polyurethane foam was fully consolidated.

The geometry of the pultruded and the sandwiched tubes are shown in Table 1. All of specimens were cut into 100mm lengths. Both ends of the tubes were kept parallel. Before the crushing test one end of tubes were triggered using a grinding machine into the shape of bevel or tulip (Figure 1).

Table 1. Geometry and dimension of the pultruded and the sandwiched composite tubes

Specimen	D_{Outer} [mm]	D_{Inner} [mm]	Outer Shell	Inner Shell	T_{Foam} [mm]
T1	51	44.6			
T2	38	31.6			
T3	25	18.6			
ST1	51	31.6	T1	T2	3.3
ST2	51	18.6	T1	T3	6.6
ST3	38	18.6	T2	T3	3.3

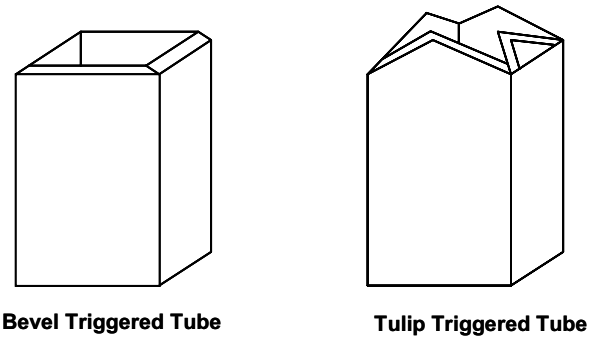

Figure 1. Geometries of bevel triggered and tulip triggered tubes

Static and Crush Tests

Static compression tests were preformed on an Instron universal test machine with a cross-head speed of 0.2mm/min. The bottom of tube was clamped during the compression testing. Load-deflection signals were recorded using a compatible PC computer. A crush test was

carried on an Instron machine at the speed of 500mm/min. The mean value of the results was obtained from a minimum of three specimens.

RESULTS AND DISCUSSIONS

Static Compression Tests

Compressive load-deformation curves of the pultruded tubes are shown in Figure 2 (left). The compression strength and modulus of the pultruded tubes decreased with an increasing ratio of square length to wall thickness. T1 tube had more failure steps before the maximum value was reached, while T2 and T3 tubes had only one failure step until the full failure. T1 tube (big square length to wall thickness ratio) mainly showed a buckling failure mode, while T2 and T3 showed a fibre and matrix fracture mode.

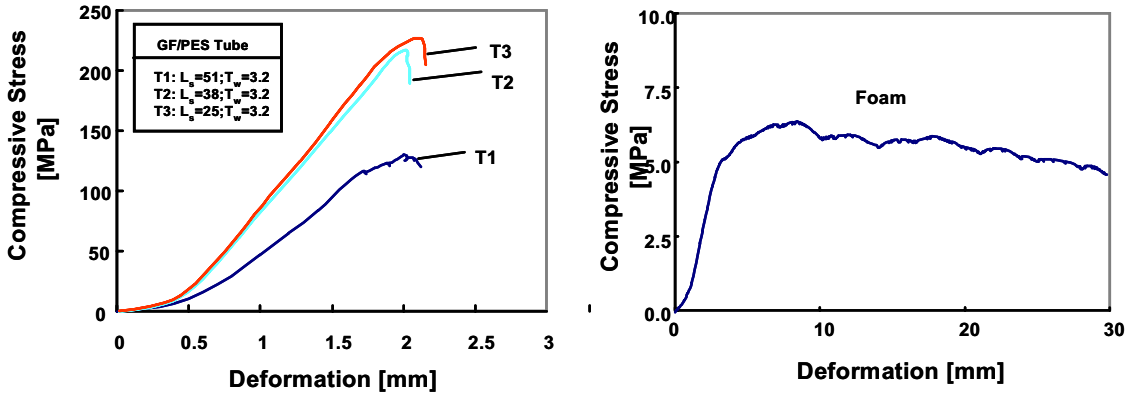

Figure 2. Compression behaviour of the pultruded tubes and the polyurethane foam

Pure polyurethane foam with a dimension of 40x40x100 mm was compression tested. The static compression load-deformations curve is shown in Figure 2 (right). The compression load reached a maximum value, then kept a nearly constant level. Cracking and collapse in the bottom of the foam was observed in the experiment. This result was quite different from the soft polyurethane foam [17] due to different densities (0.3082g/cm^3 for this foam and 0.0396g/ cm^3 for the soft foam). The compression load of the soft polyurethane foam is at a constant value in the beginning and then increased. The failure mode is a continuous fold.

Sandwiched tubes can clearly sustain higher compression loads than simple pultruded tubes, since they consist of two pultruded tubes and one layer of rigid polyurethane foam. However, the compression strength and modulus of the sandwiched tubes were lower than the pultruded tubes, because of the high content of soft foam in the sandwiched tubes (Figure 3).

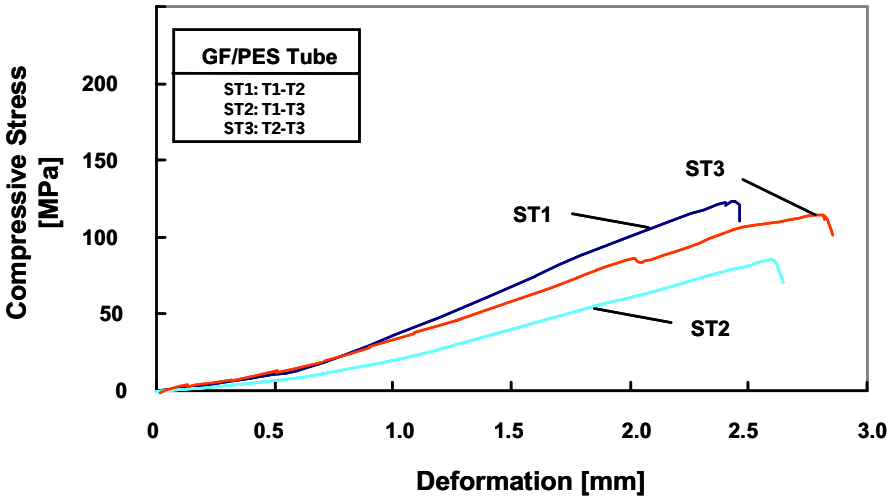

Figure 3. Compression loading-deformation curves of the sandwiched tubes

The foam volume present in ST1, ST2 and ST3 sandwiched tubes was 34.0%; 60.5% and 34.0%, respectively. ST2 had the lowest compression strength and modulus, since its foam volume fraction was the highest. The compression properties of all tubes are summarised in Table 2. The specific strength and modulus were calculated by dividing the compression strength and modulus by the global density. The specific strength and modulus of ST1 is higher than T1. If the foam volume fraction was too great, the specific strength and modulus of the sandwiched tubes were lower than those of pultruded tubes.

Table 2. Compression behaviour of the pultruded- and the sandwiched tubes

Specimen	Foam	T1	T2	T3	ST1	ST2	ST3
Maximum Compressive Load [kN]		82	82	55	201	154	121
Compressive Strength [MPa]	6.5	134	184	199	126	68	110
Compressive Modulus [GPa]	0.023	11.6	16.0	16.4	7.5	4.8	7.8
Specific Compressive Strength [10^9N.m/kg]	21.1	79.6	109.3	115.7	103.6	79.4	89.8
Specific Compressive Modulus [10^{12}m/kg]	0.075	6.9	9.5	9.5	6.2	5.6	6.4

Crush Test

The crush properties of the pultruded and the sandwiched tubes depended on the dimensions and triggered geometry shape. Two different triggered tubes (i.e. Bevel and Tulip) were studied.

A) Pultruded tubes

In the axial crushing test, the loading plate impacted first onto the sharp edges of the bevel or tulip trigger of the tube. The crush loading-deformation curves of the pultruded tubes with the bevel trigger are shown in Figure 4 (left). The load of the T1 tube had a sharp drop after to maximum value. Then the load increased and reached a stable value. The load of T2 and T3 tubes kept almost at a same constant value after reaching a maximum. Since the failure mode of T1 was buckling (as observed in the compression tests) the crush process was not as stable as T2 and T3 tubes.

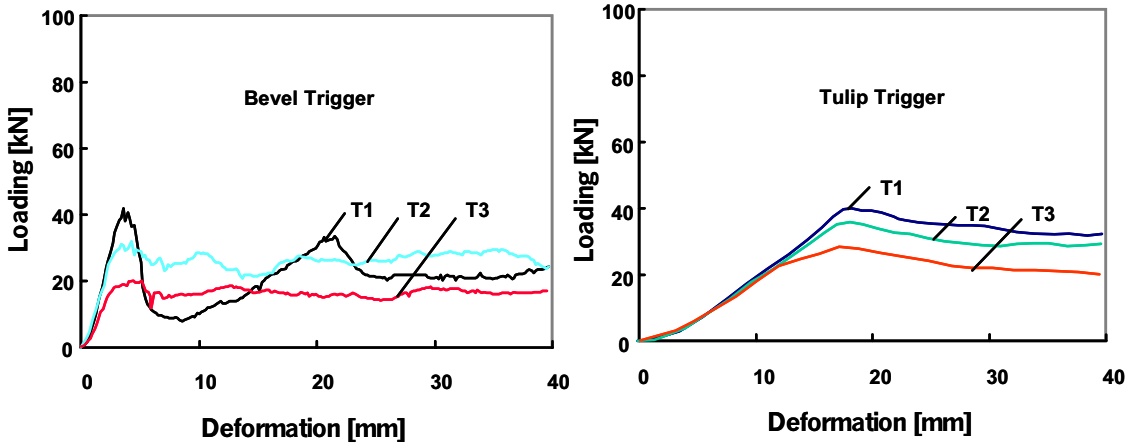

Figure 4. Crush curves of the pultruded tubes with the bevel and tulip trigger

The characteristics of loading-deformation of the pultruded tubes with the tulip trigger were quite different from the tubes with the bevel trigger (Figure 4, right). The crushing progress of the tulip triggered tube was more stable. The load of T1 increased to a maximal value then

reduced a little to a constant value. The T2 and T3 tubes had the same features. The stable average crush load of the tube with the tulip trigger can be ranked as T1>T2>T3.

The failure process of the fibre reinforced thermosetting matrix tubes were very complex. For the pultruded tube with a sharpened bevel trigger, the failure started at the inner hoop layer, consisting of a glass mat layer. The glass mat layer buckled and kinked to the inner side of the tube and delaminated at the interface of the glass mat and the unidirectional fibre layer. When the crushing continued, the outer layer of glass mat kinked and bent to the outside. In the middle of the laminate, the debris wedge made the laminate cracking propagate and delaminate along the unidirectional layers (Figure 5, left). This fracture mechanism was similar to the observation made by Thornton [6].

Tulip triggered tubes have much more fibre fracture (Figure 5, right) than the bevel triggered tube. This lead to the higher specific energy absorption in the tulip triggered tubes.

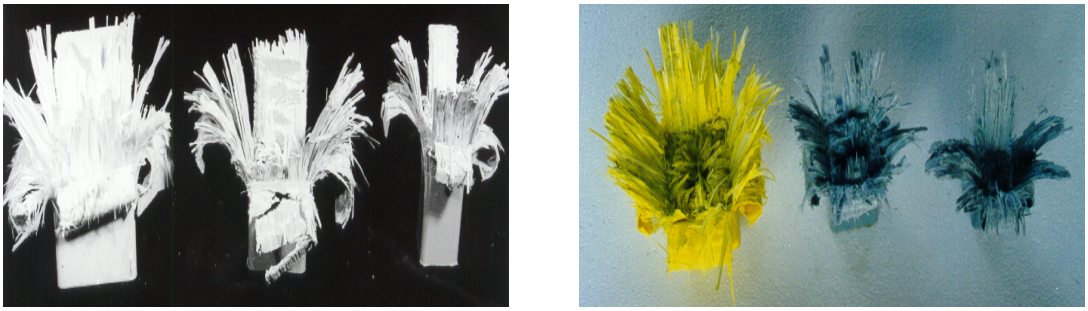

Bevel Trigger **Tulip Trigger**

Figure 5. Fracture morphology of the pultruded tubes with the bevel and tulip trigger

B) Sandwiched tubes

The sandwiched tubes with the bevel trigger had a peak load in the load-deformation curves, since the inner shell was crushed before the outer shell. During failure the first kinking point in the curve represented the failure of the inner shell. After that, the load increased continually until the failure of the total tube (Figure 6, left). Due to the thick layer of the foam, the peak load of the ST2 tube appeared relatively late. The average crush load of the sandwiched tubes can be ranked as ST1>ST3>ST2. For the sandwiched tube with the tulip trigger, the load-deformation is shown in Figure 5, right. The crush load reached the maximal value, then the crush propagated stably. The average of the crush load of the tulip trigger was higher than the bevel triggered tube.

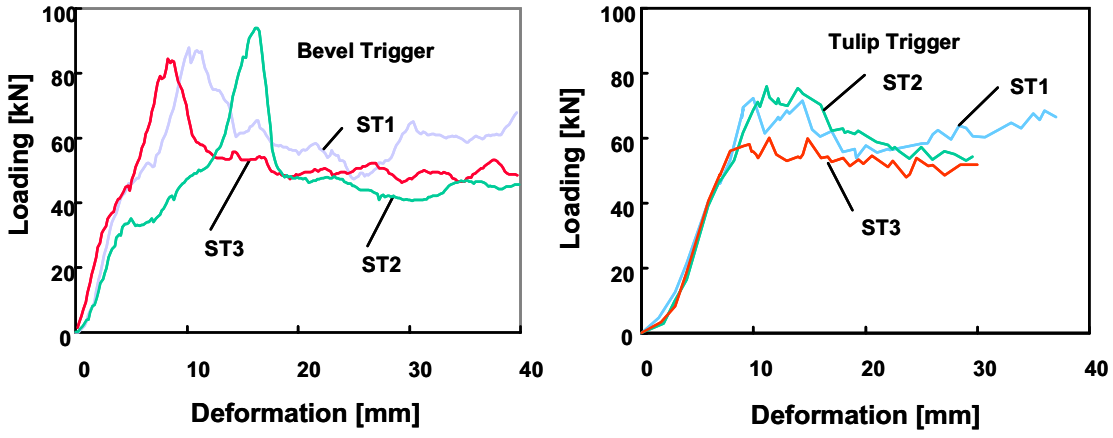

Figure 6. Crush load-deformation curves of the sandwiched tubes with the bevel and tulip trigger

The outside shell of the ST1 and ST3 tubes with both triggers had more fibre and matrix fracture (Figure 7, left). The foam was fractured into small parts. However for ST2 tube, the outside shell bent with less fracture, since the foam cracked and deformed.

The fracture morphology of the tulip triggered sandwich tubes was the same as the bevel triggered tubes after larger crush process (Figure 7, right). More fracture existed in the ST1 and ST3 tube than the ST2 tube.

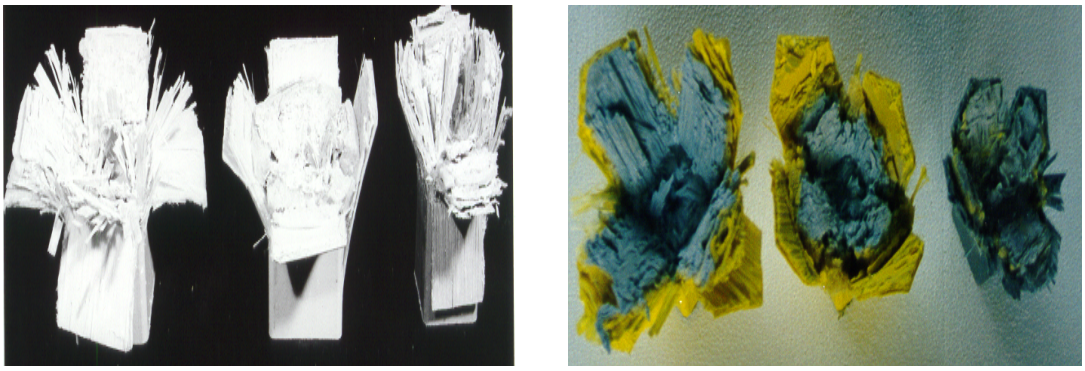

Bevel Trigger **Tulip Trigger**

Figure 7. Fracture morphology of the sandwiched tubes with the bevel and tulip triggers

For sandwiched tubes, the trigger geometry was not as sensitive as the pultruded tube in the crush process. (Figure 8, left) The surface layers of the outer shell kinked and bent similarly as the pultruded tubes. However the inner side of the outer shell was more kinked and fractured, since the rigid foam restricted the bending of the inner side layer. Between the glass mat and the unidirectional fibre lays a large delamination was observed. The unidirectional fibre bond had been spoliated into more branches. The outside layer of the inner shell broke to small debris, as it had with the inner side layer of the outer shell tube. The inner side of the inner shell tube was continually kinked and fractured.

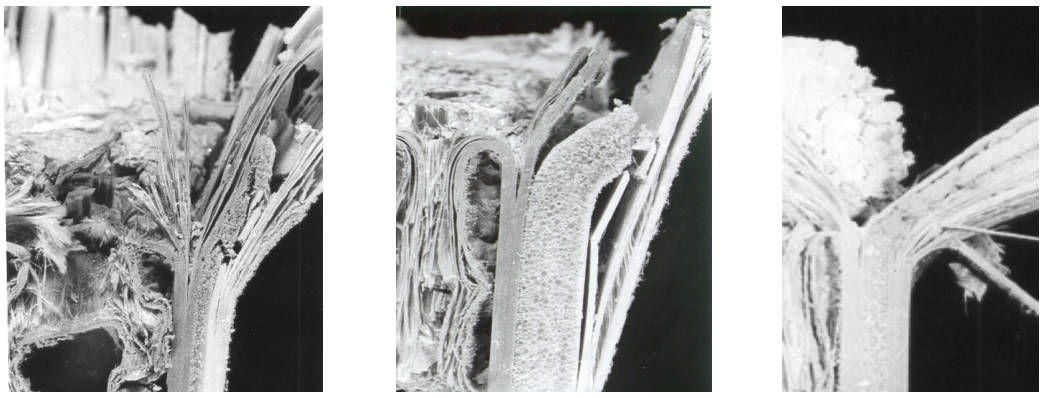

ST1 **ST2** **ST3**

Figure 8. Fracture morphology of sandwiched tube with the tulip trigger

Since ST2 had a thicker foam layer than ST1 the fracture modes was totally different. (Figure 8, middle). The very large delamination happened between the outer shell and the foam layer. The outer side layer of the outer shell only had a few kinks and fractures. The delamination between the glass mat and the unidirectional layer was mainly damaged in the outer shell. In the inner shell, the outer side layer of the inner shell fracture into small parts while the inner side of tube kinked and continued bending.

The ST3 specimen (Figure 8 right) had a delamination only in the outer shell tube between the glass mat and the unidirectional layers. The main fracture was in the corner and the crack length was much longer than the crush distance. Since this crack was in the corner, the outer shell bent with little fracture. This phenomenon can be observed in both the triggers. The inner shell showed the same fracture mode as the ST1.

Specific energy absorption

The specific energy absorption was an indicator for the crush properties of the crashworthy materials. For both bevel and tulip triggered pultruded tubes, the specific energy absorption of both the T2 and T3 tubes was clearly higher than that of the T1 tube. The energy absorption capability increased with the ratio of the square length to wall thickness. The specific energy absorption of the pultruded tube also depended on the trigger geometry. The tulip triggered tube possessed higher energy absorption than the bevel triggered tube, since more fibre fracture occurred in the crush propagation (Figure 9).

For the sandwiched tubes the specific energy absorption ability is independent of the trigger shapes. The specific energy absorbing capability of sandwiched tubes can be ranked as ST3>ST1>ST2.

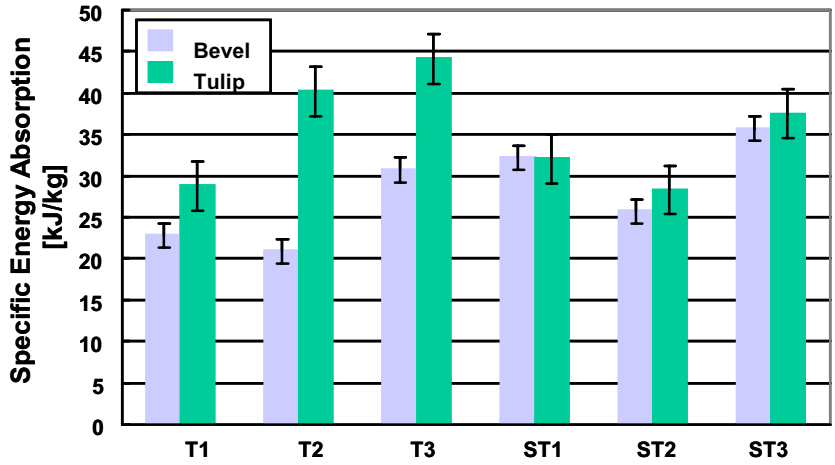

Figure 9. Specific energy absorption of the pultruded- and the sandwiched tubes

CONCLUSIONS

The sandwiched tubes consisting of pultruded tubes and a rigid polyurethane foam can be useful as crashworthy components. The fracture mechanism of the pultruded tube depended on the triggered geometry. The tulip triggered tube showed higher crush load and more stable crush process than the bevel triggered tube. All of the sandwiched tubes showed stable crushing process for both triggered tubes. The thin foam layer has a better effect than the thick foam, since the thick foam produced a larger delamination fracture between the shell tubes and the foam layer.

REFERENCES

1. Hull D. A unified approach to progressive crushing of fibre-reinforced composite tubes, Compos. Sci. Techno., **40** (1991) pp. 377-421.
2. Thornton P. H. & Edwards P. J. Energy absorption in composite tubes, J. Compos. Mat., **16** (1982) pp. 521-45.
3. Hamada H. & Ramakrishna S. Effect of fibre material on the energy absorption behaviour of thermoplastic composite tubes, J. Thermopl. Compos. Mat., **9** (1996) pp. 259-79.

4. Price J. N. & Hull D. Axial crush of glass fibre-polyester composite cones, Compo. Sci. Techno., **28** (1987) pp. 211-30.
5. Karbhari V. M. Energy absorption characteristics of hybrid braided composite Tubes, J. Composite Materials, 31, (1997), 1164-1186
6. Thornton P. H. Energy absorption in composite structures, J. Compo, Mat., **13** (1979) pp. 247-62.
7. Thornton P. H. The crush behaviour of glass fiber reinforced plastic sections, Compos. Sic. Techno., **27** (1986) pp. 199-223.
8. Farley G. L. Energy absorption of composite materials, J. Compos. Mat., **17** (1983) pp. 267-79.
9. Ramakrishna S., Hamada H., Makawa Z. & Stao H. Energy absorption behavior of carbon-fibre reinforced thermoplastic composite tubes, J. Thermopl. Compos. Mat., **8** (1995) pp. 323-45.
10. Farley G. L. Effect of fiber and matrix maximum strain on the energy absorption of composite materials, J. Compos. Mat., **20** (1986) pp. 323-34.
11. Farley G. L. Crushing characteristics of continuous fiber-reinforced composite tubes, J. Compos. Mat., **26** (1992) pp. 37-50.
12. Fleming D. C. and Vizzini A. J. The effect of side loads on the energy absorption of composite structure, J. Compos. Mat., **26** (1992) pp. 486-99.
13. Mamalis A. G. and Manolakos D. E. Crashworthy behaviour of thin-walled tube of fibreglass composite materials subjected to axial loading, J. Composite Materials 24, (1990), pp. 72-91.
14. Czaplicki M. J., Robertson R. E. & Thornton P. H. Comparison of bevel and tulip triggered pultruded tubes for energy absorption, Compos. Sci. Techno., **40** (1991) pp. 31-46.
15. Sigalas I, Kumosa M. and Hull D. Trigger mechanisms in energy-absorbing glass cloth/epoxy tubes, Composites Science and Technology, 40, (1991), pp. 265-287.
16. Farley G. L. Effect of specimen geometry on the energy absorption capability of composite materials, J. Compos. Mat., **20** (1986) pp. 390-400.
17. Thornton P. H. The crush behaviour of pultruded tubes at high strain rates, J. Compos Mat., **24** (1990) pp. 595-615.
18. Czaplicki M. J., Robertson R. E. & Thornton P. H. Non-axial crushing of E-glass/polyester pultruded tubes, J. Compos. Mat., **24** (1990) pp. 1077-100.
19. Gupta N. K., Velmurugan R. and Gupta S. K. An analysis of axial crushing of composite tubes, J. Compos. Mat., **31** (1997) pp. 1262-86.
20. Wei S. Performance of new sandwich tube under axial loading: experiment, J. Structural Eng., **121** (1995) pp. 1806-14.
21. Wei S. Performance of new sandwich tube under axial loading: analysis, J. Structural Eng., **121** (1995) pp. 1815-21.